DOI: 10.55522/jmpas.V11I1.1389 ISSN NO. 2320–7418

International peer reviewed open access journal

Journal of Medical Pharmaceutical and Allied Sciences

Journal homepage: www.jmpas.com CODEN: JMPACO

Research article

Design and characterization of daunorubicin loaded solid lipid nanosuspension

N Dora Babu

College of Pharmacy, Uruk University, Baghdad, Iraq

ABSTRACT

Objective the objective of the current review was to research the conceivable utilization of strong lipid nanosuspension (SLNs) as a medication conveyance strategy to support Daunorubicin (DNR) mind focusing on execution after intranasal (I. n.) organization. Techniques: 33 factorial plans were applied for advancement by utilizing lipid fixation, surfactant focus, and High-speed homogenizer (HSH) mixing time as reliant factors, and their impact was seen on particles size, Polydispersity record (PDI), and entanglement proficiency. Results with the organization of Compritol® 888 ATO (4.6 % w/v), tween 80 (1.9 % w/v), and HSH blending time, the enhanced equation DNR-SLNs arranged (10 min). Molecule size, PDI, zeta potential, capture effectiveness, percent in vitro discharge was viewed as 167.47±6.09 nm, 0.23±0.02, 24.1 mV, 75.3±2.79, and 89.35±3.27 percent in 24 h, individually, for streamlined detailing (V-O). No significant changes in molecule size, zeta potential, and ensnaring effectiveness were found in the security learns at 4±2 °C (fridge) and 25±2 °C/60±5% RH up to 3 mo. Conclusion following the administration of non-invasive nose-brain drugs, which is a promising therapeutic strategy, the positive results confirmed the current optimized formulation of DNR-loaded SLNs.

Keywords: Solid lipid Nanosuspension, Homogenization and Ultrasonication, Characterization, Factorial design, Nose to brain delivery.

Received: 16-06-2021, Accepted: 21-12-2021

Correspondence: Dr N Dora Babu* ✉ ndorababu81@gmail.com

College of Pharmacy, Uruk University, Baghdad, Iraq

INTRODUCTION

Presently, the most generally utilized malignant growth therapy is through chemotherapy directed either by the intravenous or oral course, which hurts the ordinary cells something other than the carcinogenic cells in the body and causes numerous undesirable incidental effects [1].

Daunorubicin hydrochloride (DNR) is a wide range anthracycline anticancer medication administrated intravenously, including the US Food and Drug Administration (USFDA) endorsed pegylated liposomal Daunorubicin showcased as DNRil® for therapy of various human diseases [2-4]. No huge improvement in effectiveness has been found through investigations in spite of the utilization of DNRil® because of languid and inactive arrival of the medication [5].

Treating mind sicknesses utilizing hydrophilic medications like DNR is yet more troublesome as Blood-Brain Barrier (BBB) confines the section of medication and forestall their take-up in the cerebrum. Because of BBB, no huge atom can arrive at the mind and under 2% of little particles track down a section in the cerebrum, making a group in the therapy of numerous hazardous cerebrum sicknesses, including cerebrum malignant growth [5]. Intranasal organization is a harmless way that can convey tranquilizes straightforwardly into the cerebrum, bypassing BBB through the trigeminal or olfactory pathway. It has been taken advantage of by analysts, trailed by the upsides of self-medicine, ease conveyance, turn away first-pass digestion, fast beginning, decrease in portion sum when contrasted with oral course [6].

Nanoparticulate-based medication conveyance might further develop the medication conveyance to the cerebrum through nasal course. These frameworks shield the medication from P-glycoprotein (P-gp) efflux, compound, as well as synthetic debasement with an expansion in bioavailability and explicit biodistribution [7] Strong Lipid Nanoparticles (SLN) is a submicron lipidic transporter ensnaring the medication in the lipid center and balanced out with the guide of surfactant, co-surfactant, and additionally stabilizer.

The destinations of the current review were to apply an exploratory plan approach in the improvement of DNR-stacked SLN conveyance managed through nasal course. The exploratory plan was applied to improve the autonomous factors (Concentration of Compritol 888 ATO, Concentration of tween 80, and High-Speed Homogenizer time) to accomplish low molecule size, low polydispersity list (PDI), and high capture productivity (EE). DNR SLN were figured out, enhance, and were portrayed for physicochemical, morphological, in vitro discharge, and motor instruments [8, 9].

MATERIALS AND METHODS

DNR was gathered from Amneal Pharmaceuticals Ltd (Ahmedabad, India) as a gift test. Apifil, Compritol 888 ATO, Compritol HD5 ATO, Capryol 90, and Precirol ATO 5 (PA) were gathered as gift tests from Gattefosse Pvt. Ltd. (Mumbai, India). Stearic corrosive, Tween 80, and Poloxamer-407 (Pol-407) were secured from Sigma-Aldrich (Bangalore, India). Hydrogenated soybean phosphatidylcholine (HSPC) 50 was gathered from the Sun Pharma Advanced Research Center (SPARC, Vadodara) as a gift test.

Selection of lipid using Solubility study of DNR in different lipids

Lipid determination is one of the main elements in Solid Lipid Nanosuspension in choosing the medication's exemplification execution in the lipid. The DNR dissolvability examination has been researched in five distinct lipids viz. Compritol 888 ATO, Compritol HD 5 ATO, Precirol ATO 5, Apifil, Stearic corrosive for deciding their capability to solubilize DNR. The solvency couldn't be evaluated by the balance method since the vast majority of the lipids utilized were in strong condition. Consequently, an elective methodology was utilized, where DNR (20 mg) was set in five separate vials. The lipids were independently warmed over their softening point and continuously added to the vials until a reasonable arrangement of lipids is shaped. The trial was acted in three-fold [10].

Formulation of DNR loaded SLN

SLN was formed utilizing the course of homogenization and ultrasonication. The methodology was comprise of taking lipid and medication in one section while a watery arrangement of surfactant and stabilizer in another part. Medication and lipid blend were liquefied over the softening mark of lipid. A fluid part was warmed at a similar temperature. When both the parts accomplish a balance, a fluid piece was added joined into the lipid stage, trailed by emulsification by a rapid homogenizer. The temperature of the blend was kept up with consistent until complete emulsification happens. Subsequent to acquiring essential emulsion, the combination was ultrasonicated utilizing an Ultrasonic homogenizer (Probe sonicator) (orchid logical and imaginative India Pvt ltd, Ambad, Nashik) to get Solid lipid-based Nanosuspension (SLNS).

Optimization of variables by applying factorial design

33 exploratory plan was utilized for the improvement and assessment of the connection between the autonomous factors [critical process boundaries (CPP)] viz., X1= lipid focus, X2= surfactant fixation, and X3= High-Speed Homogenizer (HSH) time and ward factors (reactions) [Critical Quality Attribute (CQA)], for example, Y1= Particle size, Y2= Polydispersibility file (PDI) and Y3= % Entrapment proficiency (EE) (table 1). Here, Compritol 888 ATO, Tween 80, and poloxamer 407 were chosen as lipid, surfactant, and stabilizers, individually. Drug fixation (2 mg/ml), HSH speed (10000 rpm) and Poloxamer-407 focus (1% iw/w), sonication sufficiency (20%) were set as fix levels.

Utilizing Design Expert programming (Version 12.0, Stat-ease. Inc., US), the factorial plan was assessed and a polynomial condition was gotten. In the polynomial condition, the size of the coefficients has positive signs showing a reliable result or a negative sign demonstrating a differentiating impact. The most fitting test model (harmony, a blend of two, quadratic and cubic model) was resolved in light of the correlation of factual boundaries like the coefficient of variety (CV), the coefficient of augmentation (R2), the different coefficients of amendment changed (R2 changed), the square lingering total anticipated and the 3D reaction surface plot given by Design-Expert programming graphically. The degree of importance was considered at a p-esteem <0.05.

Table 1: Selection of variable and their level

Factor (Independent variable)	Levels		
	Low (-1)	Middle (0)	High (+1)
X1= Compritol ATO 888 (as a lipid) concentration (%w/w)	3	4	5
X2 = Tween 80 concentration (%w/w)	1.5	2	2.5
X3=HSH Time (min)	5	10	15
Response (Dependent variable)	Goals		
Y1= Particle size	Minimize		
Y2= PDI	Minimize		
Y3= % iEE	Maximize		

Data optimization and model validation

To create a design space to ensure the quality of the product you want, the impact of each independent CPP on CQA was analysed. 33 factorial design is used in the design space proposal to examine process parameters, the answer to the quality attributes of DNR SLNs is used. The optimization is carried out using an overlay plot (graphical) and desirability (numerical) parameters based on finding the particle size, PDI, and higher EE percentage.

Characterization of optimized DNR-SLNs

For portrayal, streamlined DNR-SLNs were formed and they were described for physicochemical, morphological, in vitro drug discharge, and motor investigations as displayed underneath:

Similarity investigation of lipid and medication

The similarity study between the chose lipid and medication was performed by utilizing a Fourier change infrared Spectro-photometer (FTIR) and Differential examining calorimetry (DSC).

Fourier change infrared spectrophotometer (FTIR)

FTIR spectroscopy of Daunorubicin hydrochloride, unadulterated lipid excipients, and actual combination (DNR+lipid) was performed utilizing the Fourier change infrared spectrophotometer (Alpha-model Bruker ATR FTIR spectrophotometer). Spectra were examined at a goal of 4 cm-1 over a frequency locale of 4000 to 400 cm-1. The cycle comprised of scattering KBr tests and compacting them into plates by applying a water powered press strain of 5 tons for 5 min (KBr pellet strategy). In the light course, the pellet was situated and the range was gathered.

Differential checking calorimetry (DSC)

DSC estimation of Pure Drug Daunorubicin (DNR), Pure Lipid excipients and Physical combination (DNR+Lipid), clear (fake treatment) SLNs, and DNR stacked SLNs definition was performed with an instrument (Perkin-Elmer Diamond DSC) for estimation of the thermotropic change of lipids. Void aluminium dish was utilized as reference and tests were painstakingly positioned in another aluminium container. The estimation was done in an idle climate inside the temperature scope of 30 °C to 200 °C, at 5 °C per min.

X-beam diffraction (XRD)

The crystallographic construction of DNR, Compritol 888 ATO, the actual combination (drug+lipid), clear SLNs, and DNR-SLNs were described by X-beam diffraction (XRD) (D8Advance; Bruker Optik GmbH, Ettlingen, Germany). Tests were presented to Cu-Ka radiation (40 kV; 40 mA) at an output pace of 0.02 °/second over the 2θ/minute scope of 5°-50°.

Molecule size and polydispersity file (PDI) and zeta potential

Photon connection spectroscopy (PCS; Zetasizer, HAS 3000; Malvern Instruments, Malvern, UK)) was performed to decide molecule size and Polydispersity Index (PDI). DNR SLNs are weakened multiple times with twofold refined water

$$\%EE = \frac{\text{Total amount of DOX} - \text{Amount of free DOX}}{\text{The total amount of DOX}} \ldots\ldots\ldots \text{eq (1)}$$

prior to estimating the size and PDI. Estimations of molecule size and PDI were completed by taking 1 ml of the weakened detailing into polystyrene cuvettes and dispensable collapsed narrow cells at 25 °C, individually, for zeta potential. At a frequency of 633 nm, dynamic light dissipating estimations were taken utilizing the helium-neon laser as a light source at a dispersing point of 90o, where molecule dissemination is changed into molecule size because of Brownian movement. On account of zeta potential, particles travel with a speed connected with their zeta potential because of the use of an electric field, which is resolved utilizing a method called stage investigation light dissipating and changed over to the zeta potential by inbuilt programming.

Morphological portrayal of upgraded DNR SLNs

Transmission electron microscopy (TEM) (JEM-1200, JEOL Co. Ltd., Tokyo, Japan) was utilized to envision the surface morphology of the formed nanosuspension. A drop of the nanoparticles scattering was finely spread on a copper framework covered carbon with films and contrarily stained with 2% (w/v) phosphotungstic corrosive for review [11].

A pH of streamlined DNR SLNs

By taking 10 ml of detailing in a measuring glass, the pH of the DNR-stacked not set in stone. At room temperature, pH was estimated utilizing an aligned computerized pH meter (Eutech Instruments, pH coach, Singapore)

The thickness of advanced DNR SLNs

To concentrate on the Rheological conduct of the SLNs plan was resolved utilizing Brookfield viscometer (Expert L series, Fungilab Brookfield viscometer). Thickness conclusions were performed at 50 rpm utilizing shaft TL6 at 25±2 °C.

Entrapment efficiency (%EE) of DNR SLNs formulated batches

The percent EE of formulated DNR SLNs was calculated using the method of centrifugation. To obtain lipid nanoparticles, samples were collected in centrifuge tubes and centrifuged at 10000 rpm for 20 min at room temperature. The supernatant was obtained, diluted with methanol appropriately, and analysed by UV spectroscopy for free drug material. %EE was calculated by following equation (1) [12].

***In vitro* drug release of optimized DNR SLNs and release kinetics mechanism**

Using a dialysis bag diffusion technique, *in vitro* drug release was assessed. A total of 5 ml of the sample was taken into a dialysis bag and submerged in a beaker containing 200 ml of phosphate-buffered saline (pH 7.4) at 37±1 °C for 12 h with continuous stirring using a shaking incubator at a speed of 100 rpm (REMI Instruments Ltd). An aliquot of 1 ml of dissolving medium was removed at a fixed interval and the same volume of fresh medium was applied. Then the absorption of withdrawn samples was measured at 480 nm against a blank reagent using the UV spectrophotometer (Agilent Cary 60 UV-Vis spectrophotometer). Throughout the experiment, sink conditions were preserved.

All the experiments were performed in triplicate. The data obtained from the *in vitro* drug release analysis were adapted to various kinetic models viz., zero-order (cumulative drug release percentage versus time), first-order (cumulative drug release log remaining versus time), Higuchi model (cumulative drug release percentage versus square root of time) Hixon Crowell model (cumulative drug root remaining versus time) and Korsmeyer-Peppas model (Log percent CDR versus log time) [13].

RESULTS AND DISCUSSION

The solubility of DNR in lipids

A limiting factor in the formulation of SLNs is the amount of solid lipid needed to solubilize the drug. In Solid lipid nanosuspension formulation, the amount of lipid required to solubilize the drug is a crucial factor as it has a significant impact on the % entrapment efficiency. As per the details shown in fig. 1, to conduct the solubility analysis, five distinct solid lipids were taken. DNR solubility in Compritol 888 ATO required a lower quantity, suggesting higher drug solubility. As it has been successfully used in various pharmaceutical dosage types, Compritol 888 ATO has attracted particular interest. The applicability of Compritol 888 ATO in the preparation of aqueous colloidal dispersions such as solid lipid microparticles (SLMs), solid lipid nanoparticles (SLNs) and

nanostructured lipid carriers (NLCs) to capture lipophilic drugs has been highlighted in various research studies [14-20].

33 factorial design

A significant and critical problem in the production of pharmaceutical dosage forms is the investigation of an ideal formula for the design of medication of the desired quality through minimum trials within a short period. In the literature on the development of different pharmaceutical dosage types, optimization through computer-aided statistical experimental design methodologies has been successfully applied. The technique of statistical optimization involves designing a series of experiments that will calculate the response variables accurately, fitting the data with mathematical models, performing sufficient statistical tests to choose the best possible model, and producing an optimal response; the values of independent formulation variables are calculated. A factorial design is one of the common experimental designs used in the optimization of formulations between different statistical designs.

Selection of factors, levels, and Responses of experimental design

33 factorials were developed to analysed the main effect, the interaction effect, and the quadratic effect of three independent variables (CPP) on the three responses (CQA). Here, 30 experiments run were performed, and the results were shown in Table 2.

Table 2: Observed response for size, PDI, and % EE of factorial runs

Run	X1	X2	X3	Y1	Y2	Y3
VS1	3	1.5	5	252.5±5.29	0.32±0.074	52.1±2.13
VS2	4	1.5	5	239.1±4.87	0.291±0.022	58.5±1.89
VS 3	5	1.5	5	279.7±3.43	0.327±0.03	62±1.11
VS 4	3	2	5	218.9±6.55	0.306±0.051	54.6±2.56
VS 5	4	2	5	200.6±4.11	0.257±0.029	64±2.44
VS 6	5	2	5	239.2±5.01	0.325±0.04	71.7±1.21
VS 7	3	2.5	5	279.2±3.72	0.361±0.036	47.1±1.35
VS 8	4	2.5	5	285.3±4.36	0.35±0.064	51.2±2.47
VS 9	5	2.5	5	306.8±5.63	0.393±0.02	61.6±3.12
VS 10	3	1.5	10	188.2±3.08	0.235±0.05	57.4±2.40
VS 11	4	1.5	10	165.3±3.51	0.211±0.047	67.2±1.39
VS 12	5	1.5	10	228.5±4.13	0.27±0.059	73.1±2.78
VS 13	3	2	10	174.4±5.29	0.25±0.067	65.2±3.29
VS 14	4	2	10	142.5±2.05	0.201±0.018	74.2±2.87
VS 15	5	2	10	199.4±1.33	0.278±0.083	79±1.55
VS 16	3	2.5	10	208.2±2.58	0.307±0.077	52.7±2.31
VS 17	4	2.5	10	222.1±4.77	0.318±0.045	58.7±3.33
VS 18	5	2.5	10	239.6±6.63	0.299±0.089	67.5±3.59
VS 19	3	1.5	15	196.1±5.97	0.423±0.049	43.1±3.54
VS 20	4	1.5	15	183.9±6.28	0.401±0.09	49.4±2.65
VS 21	5	1.5	15	246.7±8.39	0.451±0.057	59.8±2.48
VS 22	3	2	15	191.2±3.99	0.385±0.03	45.2±1.66
VS 23	4	2	15	171.4±9.25	0.36±0.063	53.5±2.09
VS 24	5	2	15	225±4.58	0.40±0.087	62±2.98
VS 25	3	2.5	15	248.7±6.89	0.441±0.091	39.8±3.23
VS 26	4	2.5	15	261.2±7.15	0.465±0.05	47.2±2.29
VS 27	5	2.5	15	251.1±4.92	0.446±0.028	55.4±1.73
VS 28	4	2	10	137.3±7.50	0.187±0.07	77.2±1.19
VS 29	4	2	10	148±6.25	0.20±0.062	73.6±1.47
VS30	4	2	10	143.2±4.10	0.208±0.07	71.7±1.56

Data represent mean±SD, n=3

A quadratic model was fitted into the data of experimental results by the use of Design-Expert® Software Version 12. The Cubic model is aliased. Quadratic models were found to be best fit models for all dependent variables *viz.*, size, PDI, and %EE, and the R2values for the quadratic model were found to be 0.9339, 0.9095, and 0.9035 whereas for the cubic model R2 values were 0.7147, 0.8376 and 0.7444 respectively. These models were evaluated statistically by applying one-way ANOVA ($p<0.05$). The result of the ANOVA is shown in table 4

Effect of the independent variable on particle size

The particle size of factorial runs varied between 137.3 to 306.8 nm as shown in the counterplot and 3D response plot in Figure 2 and 3.

The polynomial equations for size

$$\text{Size} = +145.46 + 13.90A + 16.97B - 18.57C - 6.96AB - 0.1444AC + 0.6196BC + 28.53A^2 + 39.95B^2 + 45.73C^2 \quad \text{----------equation-2}$$

Where A, B, C, AB, AC, BC, A2, B2, C2 in Equation (2) were significant model terms.

As displayed in condition 2, Positive coefficients of component A, B, AC, BC, A2, B2, C2 indicates synergistic impact on molecule size, while negative coefficients of C, AB signifies opposing impact on molecule size. The Predicted R2of 0.9339 was in sensible concurrence with the changed R2 of 0.9833, demonstrating the sufficiency of the model to anticipate the reaction of molecule size.

Impact of lipid fixation on molecule size

It was seen that Conc. of Compritol 888 ATO (lipid focus) positively affected molecule size (Y1). It was additionally seen that as lipid focus expanded, the scattered stage thickness likewise expanded, bringing about higher-size molecule agglomeration and diminished homogenization capacity.

Impact of surfactant fixation on molecule size

According to results displayed in table 2 for different trial runs, as the convergence of tween 80 (Surfactant focus) expanded from 1.5% to 2.5% w/w, the size was diminishing and afterward with 2.5, it is expanded. With expanding grouping of tween 80 from 1.5 % to 2.5 % w/w, it showed diminished interfacial strain among lipid and fluid stage, which might control the accumulation of lipid molecule by working with the molecule parcel subsequently bringing about lower size. Higher surfactant fixations, as recorded in past examinations, successfully settle the lipid framework by shaping a steric boundary on its surface, in this way forestalling collection. When 2.5 % w/w tween 80 was utilized, the size was continually expanding, it was noticed. This was on the grounds that the alkyl chain of the surfactant atom covers the lipid molecule surface through hydrophobic connection to shape a steady lipid framework during the homogenization interaction. When this steady network has been shaped, an overabundance surfactant can make surfactant particles aggregate on the outer layer of the steady lipid lattice, causing an expansion in size for our situation.

Impact of HSH time on molecule size

Homogenization was performed at 10000 RPM for three different time spans viz., 5, 10, and 15 min. with an expansion in HT from 5 to 10 min, the size was progressively diminishing, while at 15

min size was expanding. One of the significant methods for applying motor energy to accomplish a lower size is the speed and season of homogenization for which it is utilized. Applying high motor energy for longer periods can prompt precariousness of the lipid structures created, bringing about bigger particles being totalled and shaped. As opposed to 10 min of HT, the size was higher at 5 min because of insufficient homogenization. An ideal homogenization time would thusly add to the making of stable particles with a uniform dissemination of size.

Impact of the free factor on PDI

As displayed in the counterplot and 3D reaction plot in fig. 2 and 3, the PDI of factorial runs went from 0.187 to 0.465.

The polynomial conditions for PDI were according to following;

PDI = + 0.2057+0.0082A+0.0230B+0.0460C-0.0064AB-0.0027AC-0.0104BC+0.0337A2+0.0427B2+0.1145C2- - - - ----------condition 3

Where A, B, C, AB, AC, BC, A2, B2, C2 in Equation (3) were critical model terms. Positive coefficients of variables A, B, C, A2, B2, C2 indicate synergistic impact on PDI as displayed in condition 3, while negative coefficients of element AB, BC, AC mean opposing impact on PDI. The anticipated R2 0.9095 was in great concurrence with the adjusted R2 0.9323, demonstrating the sufficiency of the model for foreseeing PDI.

As far as genuine factors, the condition can be utilized to make forecasts of the solution for each component at given levels. Here, for each variable, levels ought to be characterized in the first units.

To compute the overall effect of each element, this condition ought not be utilized on the grounds that the coefficients are scaled to fit the units of each variable and the block isn't at the focal point of the plan space.

Impact of lipid fixation on PDI

It was seen that Conc. of Compritol 888 ATO (lipid fixation) positively affected PDI (Y2). It was likewise seen that as lipid fixation expanded, the scattered stage thickness additionally expanded, coming about in more noteworthy PDI because of molecule agglomeration and decreased homogenization capacity.

Impact of surfactant fixation on PDI

According to the outcomes displayed in table 2 for various trial runs, PDI diminished as the grouping of tween 80 (surfactant fixation) expanded from 1.5 % to 2.5 % w/w. With an expanded grouping of tween 80 from 1.5 to 2.5 % w/w, diminished interfacial strain among lipid and fluid stage was displayed to manage lipid molecule total by working with molecule parcel, bringing about lower PDI. It was seen that PDI expanded persistently when 2.5 % w/w tween 80 was utilized,

Impact of HSH time on PDI

For three separate time spans, viz., 5, 10, and 15 min, homogenization was performed at 10000 RPM. PDI diminished steadily with an increment in HT from 5 to 10 min, while PDI expanded step by step at 15 min.

Impact of the free factor on % entanglement proficiency (EE %)

As displayed in the counterplot and 3D reaction plot in fig. 2 and 3, the % EE of factorial runs went from 39.8 to 79.

The polynomial conditions for %EE were according to following;

% Capture Efficiency (EE %) =+72.88+7.61A-2.08B-3.63C+0.5906AB+0.8203AC+0.6073BC-0.9674A2-7.43B2-12.82C2

Equation 4

Where A, B, C, AB, AC, BC, A2, B2, C2 in Equation (4) were huge model terms.

As displayed in condition 4, the positive element A, AB, BC, AC coefficients mean a synergistic impact on percent EE, while the negative variable B, C, A2, B2, C2 coefficients signify a hostile impact on percent EE. The anticipated R2 0.9035 was in great concurrence with the altered R2 0.9324 proposed the sufficiency of the model for estimating the % EE reaction.

Impact of lipid fixation on % EE

It was seen that Conc. of Compritol 888 ATO (lipid fixation) positively affected % EE (Y3). It was likewise seen that as lipid focus expanded, the thickness of the scattered stage additionally expanded, bringing about diminished homogenization effectiveness of molecule agglomeration. The higher % EE might be because of the presence of higher lipid focuses, which give extra space to the medication atom to be imgded, hence lessening the general surface region. As the consistency of the lipid stage is higher and hence shows higher %EE, this can prompt a decrease in the dispersion pace of the solute atom. From the result displayed in table 4, it was seen that 3% lipid focus showed powerless % EE of 39.8±3.23 contrasted with 5% lipid fixation showing more than 55 % EE in all test runs since lipid amount was higher.

Impact of surfactant focus on % EE

As displayed in table 2 for various exploratory runs, as the centralization of tween 80 (surfactant focus) expanded from 1.5% to 2.0% w/w, EE percent expanded. It was observed that the percent EE was diminished when 2.5 percent w/w tween 80 was utilized. The decrease in EE percent could be because of a higher solubilization impact delivered by a higher DNR surfactant fixation. DNR solvency in the outer stage can increment at higher surfactant fixations because of the dissemination of the medication from the lipid center into the watery stage, coming about in a diminished % EE. The discoveries were predictable with the consequences of another gathering portraying a lower EE rate, which might be ascribed to the solubilization impact of the emulsifier on the fluid stage drug particle.

Impact of HSH time on % EE

The % EE was viewed as lower in 15 min than in 10 min. This was owing to the expulsion from the lipid surface of surfactant particles, which actuated lipid interruption and the departure of the caught drug into the watery cycle.

Optimization of data and validation of response surface methodology

To make new definitions with the ideal reaction (ideal quality), a mathematical advancement strategy utilizing the allure approach was utilized. The ideal scopes of in reliable (factors) were restricted to 3≤A≤5 % 1.5≤B≤ 2.5 %, and 5 ≤C≤ 15 min, while the ideal reaction ranges were restricted to 200≤Y1≤100 nm, 0.15≤Y2≤0.3, and 70≤Y3≤ 80 %. The ideal reaction esteems were acquired by mathematical examination utilizing the Design-Expert 12 programming and one of them was picked in light of the attractiveness model.

Enhanced DNR stacked Solid Lipid-based Nanosuspension (SLNs) advanced cycle variable settings proposed by configuration were arranged utilizing the homogenization and ultrasonication to assess the improvement capacity of the numerical models created by the consequences of the total 33 factorial plan.

By forming and portraying nanoparticles at the designated spot group recommended by the product, test approval of DoE preliminaries for plan factors was done. The overlay plot showing the plan space and designed boundaries as a designated spot proposed by DoE programming to get the ideal reactions is displayed in Figure 1.

Figure 1: The overlay plot indicating the region of optimal process variable settings

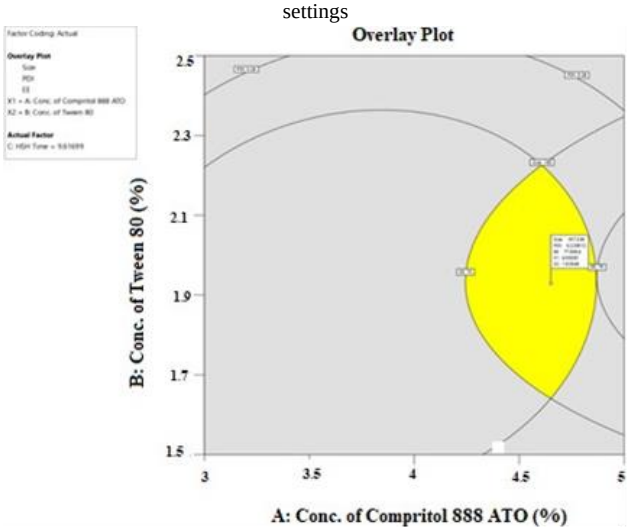

Table 3: Result of an experiment for confirming optimization capability

Code	Factor		
	Conc. of compritol 888 ATO A (%)	Conc. of tween 80 B (%)	HSH time C (Min)
V-O	4.6	1.9	10
Responses	Predicted value	aObserved Value	bResidual
Y1= Particle size (nm)	167.339	167.47±6.09	-0.12
Y2= PDI	0.220616	0.23±0.02	0.01
Y3= Entrapment efficiency (%)	77.6838	75.3±2.79	2.38

Table 4: Point prediction confirmation table

Solution 1 of 1 response	Predicted mean	Predicted median	Observed	Std Dev	n	SE pred	95% PI low	Data mean	95% PI high
Size	167.339	167.339	167.47	15.5478	3.00	10.69	145.153	167.47	189.525
PDI	0.220616	0.220616	0.23	0.0214	3.00	0.0147	0.190091	0.23	0.25114
EE	77.6838	77.6838	75.3	2.72851	3.00	1.877	73.7904	75.3	81.5773

*Interval: Two-sided, Confidence = 95%, alpha= 0.05, The observed values (particle size167.47±6.09 nm, PDI 0.23±0.02, and EE 75.3±2.79%) were comparable to the expected values (particle size 167.33. nm, PDI 0.22, and EE 77.68%) to assess the optimization procedure's reliability.

Portrayal of enhanced DNR-SLNs detailing

Fourier change infrared (FTIR) spectroscopy

The FTIR spectra over the scope of 400-4000 cm-1 for DNR, Compritol 888 ATO, and actual combination of DNR and Compritol 888 ATO are displayed in **Figure 5**.

Significant tops at 3453.59 cm-1 and 3286.90 cm-1 seemed the trademark pinnacle of NH3+Stretching, O-H extending, H-Bonding, at 2883.64 cm-1 alkane CH bunch stretch, at 1736.32 cm-1and 1728.94 cm-1 carboxylic corrosive C=O stretch, at 1173.46 cm-1 and 1104.88 cm-1 C-O extends. In the FTIR range of actual combinations of DNR and Compritol 888 ATO, these trademark pinnacles of DNR were likewise seen with practically no particular changes. This reality affirmed that no synthetic response had occurred between the medication and the polymer. Compritol 888 ATO was chosen as the lipid for planning strong lipid nanosuspension in view of a medication lipid solvency and medication lipid similarity investigation.

Differential examining calorimetry (DSC)

Similarity investigations of medication polymers are extremely fundamental before detailing plan DSC assists with giving valuable data about crystallite and amorphism of the pre-arranged example. Perkin-Elmer Diamond DSC was utilized to examine the liquefying and recrystallization conduct of the SLNs. DSC thermograms of Daunorubicin, Daunorubicin-stacked SLNs, Blank (Placebo) SLNs, actual combination (DNR and lipid), Compritol 888 ATO, are introduced in **Figure 6**.

Daunorubicin showed an endotherm relating to its MP at ~235 °C. The warm bend of the Compritol 888 ATO showed an endothermic top at ~69 °C. While, actual combination (DNR and lipid) displayed a sharp endothermic top at ~68 °C and a tiny pinnacle was found at around 234 °C, which was available in DNR. The softening endotherm of Compritol 888 ATO in clear SLNs and DNR SLN detailing was seen at 68.03 °C and 66.06 °C,

individually. DSC thermograms of an actual combination of DNR+Lipid and mass lipid displayed a liquefying endotherm relating

to the softening of DNR at ~65 °C, which was available in DNR-SLNs. Notwithstanding, the DNR top was lost in DNR SLNs. It very well may be reasoned that DNR in SLNs was in a shapeless state.

X-ray diffraction (XRD*)*

XRD patterns of DNR, Compritol 888 ATO, the physical mixture (drug+lipid), blank SLNs. and DNR-SLNs are shown in **Figure 6**.

Figure 2: IR spectra of DNR, compritol 888 ATO 88, and physical mixtures of DNR and compritol 888 ATO

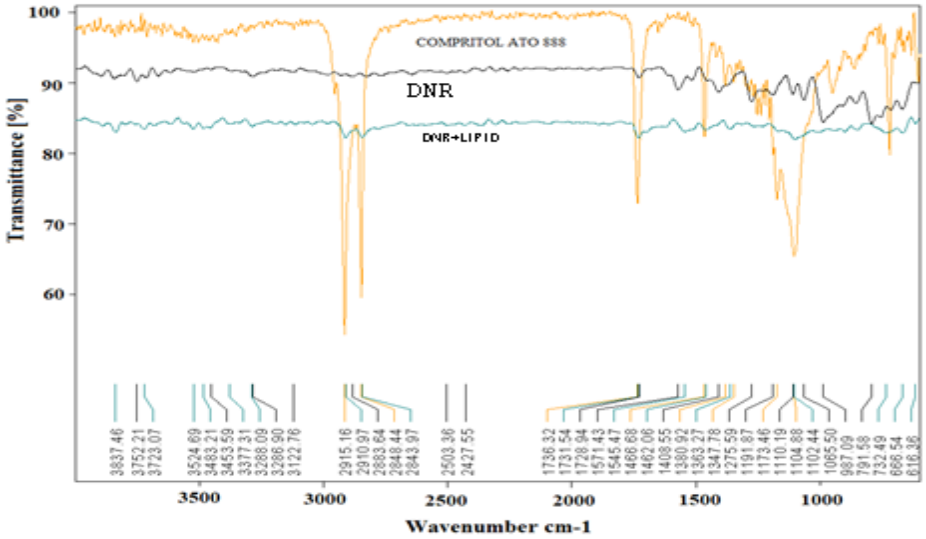

At dispersed points, DNR's XRD designs shown sharp pinnacles, going from 15° to 25°, recommending their translucent presence. Light diffraction pinnacles of DNR were seen in the actual blend at around 16 °, showing inadequate disintegration and the presence of a translucent condition of the two medications in mass lipid. The clear SLN and DNR-SLNs XRD designs were more extensive and a lot more vulnerable than the mass lipid. There were no trademark tops in DNR-SLNs for DNR, be that as it may, demonstrating the undefined province of DNR. The XRD aftereffect of these DNR-SLNs was following that of the DSC.

Molecule size, PDI, and zeta potential Molecule size dispersion and zeta expected bend of upgraded plan (V-O) were displayed in **Figure 3** (a, b), separately.

Figure 3 (a): Plot for the size distribution vs number for batch V-O (n=3)

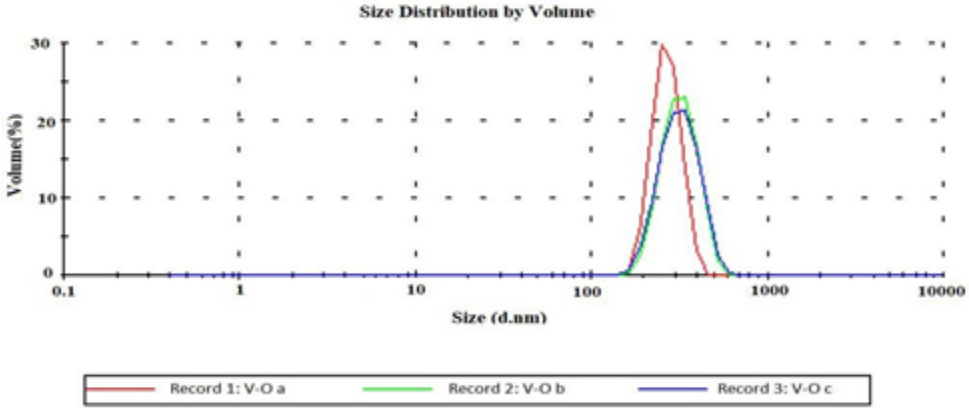

Figure 3 (b): Plot of zeta potential distribution for the batch V-O (n=3)

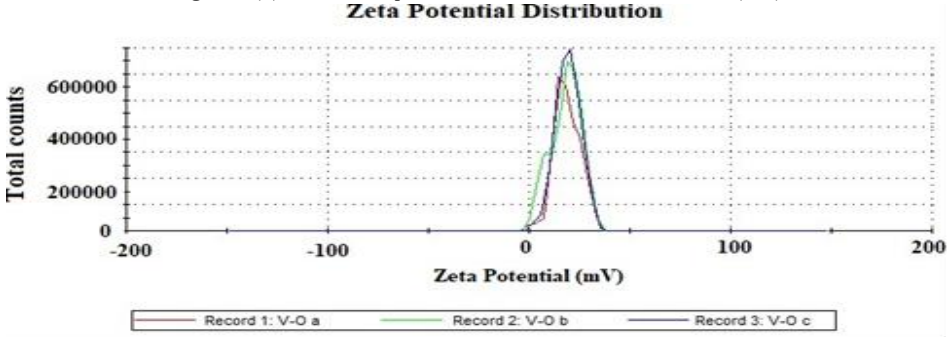

Figure 3: (a) Particle size distribution curve, (b) zeta potential curve of optimized formulation.

The average particle size of the optimized formulation was 167.47±6.09 nm, which was found to be sufficient for nasal pathway

brain targeting. In essence, PDI is the ratio of the standard deviation to the mean size of particles. A PDI value of 0.3 or less suggests particle size uniformity. In this case, the PDI value of the formed SLNs was found to be 0.23±0.02, suggesting uniformity in particle size. In the dispersion of SLNs, the zeta potential shows the degree of charge present on suspended particles. A suitably high zeta potential value (30mV to-30 mV) confers stability since aggregation is resisted by particles. The zeta potential (24.1 mV) value of the optimized formulation of SLNs showed good stability.

Morphological study

Morphological inspection of DNR SLNs using TEM analysis showed that SLNs were spherical (fig. 9) and were in the size range of 150-200 nm, which was based on the dynamic light scattering theory, in further agreement with the size distribution performed using Zetasizer.

Entanglement productivity (%)

The entanglement productivity of improved DNR SLNs plan was viewed as 75.3±2.79.

pH the improved detailing of DNR SLNs showed a pH worth of 5.86±0.35, which was inside the standard pH scope of 5-6.5 for human nasal mucosa and subsequently doesn't cause nasal irritation when directed intranasally.

Thickness

The thickness esteems for the advanced definition of DNR-stacked SLNs were 39.5±0.93 cP, which was lower than 50 cP, in this way guaranteeing solid intranasal organization resilience. Definition with a higher thickness esteem regularly brings about expanded home time yet faces organization troubles and may show diminished assimilation because of decreased medication dispersion from the detailing, though frameworks with lower consistency can be handily managed yet need to confront quicker MCC, along these lines lessening the contact season of the mucosa plan applied.

In vitro drug discharge study

A relative in vitro discharge investigation was directed between the marketed liposomal planning of DNR and the streamlined detailing of DNR-SLNs (V-O). In figure.10. the relative disintegration profile was shown. The DNR-SLNs disintegration profile showed an underlying burst discharge, trailed by a continuous delivery. The underlying burst delivery might be credited to the presence of free medications on the outer layer of particles in the outside stage and adsorbed drugs, while the sluggish delivery might be because of the embodied medication inside the lipid grid.

The advanced DNR SLNs showed an underlying arrival of 8.43±1.49 percent, contrasted with 8.13±1.52 percent after 1 h for industrially accessible DNR liposomal arrangement. Advanced DNR SLNs hence showed supported medication discharge with a combined medication arrival of 89.35±3.27 percent north of 24 h, while Marketed DNR Liposomal planning showed 94.9±4.64 percent more than 24 h. A f2 boundary is broadly used to decide the likeness of two disintegration profiles. To show the similitude between two disintegration profiles, a public standard of f2 esteem between 50-100 is utilized. For our situation, the closeness factor f2=98.33 shows that the likeness between the upgraded DNR-SLNs definition disintegration profile and the stamped DNR liposomal readiness is indistinguishable.

Analysis of kinetics and mechanism of drug release for optimized DNR SLNs

Optimized Daunorubicin-loaded lipid nanosuspension (*DNR SLNs*) formulations were fitted into various kinetic models. The correlation coefficient (R2) and exponent values of various kinetic models are shown in **Table 8**.

The outcomes showed that the motor models that could be utilized to describe the delivery attributes of Daunorubicin-stacked lipid nanosuspension (DNR-SLNs) details were more qualified to the zero-request model. The zero-request energy model had the most elevated relationship coefficients (R2= 0.982) contrasted with other motor models. Dissemination of the medication from the lipid grid has in this way been proposed to be the conceivable component of activity. The worth of delivery example "n" was viewed as 0.4597 in the Korsmeyer-Peppas model, which appears to recommend the course of delivery directed by dissemination, supposed Fickian dispersion. Comparable outcomes have been seen in Shazly, who arranged ciprofloxacin-stacked SLNs.

Table 5: Release kinetic models for the *optimized DNR-SLNs* formulation

Optimized *DNR-SLNs*	**Zero-order**		**First-order**		**Higuchi model**		**Hixon Crowell model**		**Korsmeyer–peppas**	
	R2	K0 (h–1)	R2	K0 (h–1)	R2	K0 (h–1)	R2	K0 (h–1)	R2	**n value**
V-O	0.982	3.64	0.956	0.03	0.973	21.43	0.98	0.09	0.8561	0.4597

CONCLUSION

A lipid nanoparticulate drug conveyance framework (SLNs) of Daunorubicin was proposed for cerebrum focusing through intranasal conveyance in the current exploration work. SLNs were ready by the homogenization and ultra-sonication process and assessed for molecule size, molecule size dispersion (PDI), zeta potential, capture productivity, in vitro delivery, and security studies. It was seen that all estimations were in a satisfactory reach. To plan strong lipid nanoparticles of reproducible sizes in the scope of 137.3 to 306.8 nm by tending with the impacts of handling boundaries, rapid homogenization followed by ultrasonication procedure was utilized. The 33factorial plan application ended up being a helpful strategy for enhancing DNR-stacked SLNs. Utilizing a factorial plan, the necessary definition creation can be chosen to acquire DNR-stacked SLNs more modest than 200 nm, contingent upon the use of the cerebrum focusing on framework through intranasal conveyance. The utilization of 33 full-factor plans permitted the creation of a fitting plan utilizing the

base measure of unrefined components and at least time. In vitro drug discharge more than 24 h was viewed as 89.35±3.27 percent, recommending a controlled and supported DNR-SLN discharge profile. No significant changes in molecule size, zeta potential, and ensnaring effectiveness were seen in the soundness learns at 4±2 °C (fridge) and 25±2 °C/60±5 percent RH for up to 3 mo. This review, subsequently, showed the handiness of SLNs for the conveyance of Daunorubicin through the intranasal (I. n) course to the cerebrum.

REFERENCES

1. Zubareva A, Shcherbinina T, Varlamov VP, et al, 2014. Biodistribution of Daunorubicin-loaded succinyl chitosan nanoparticles in mice injected via intravenous or intranasal routes, PCACD, 19:145-54.
2. Mussi V, Silva C, 2013. New approach to improve encapsulation and antitumor activity of Daunorubicin-loaded in solid lipid nanoparticles, Eur. J. Pharm. Sci, 48:282-90.
3. Oliveira S, Mussi V, 2016. α-Tocopherol succinate improves encapsulation and anticancer activity of Daunorubicin-loaded in solid lipid nanoparticles, Colloids Surf B, 140:246-53.
4. Lala RR, Shinde AS, Nandvikar NY, 2018. Solid lipid nanoparticles, a promising approach for combinational drug therapy in cancer, Int J Appl Pharm, 10:17-22.
5. Xiong P, Ding A, Su Z, et al, 2015. The efficacy and hyperthermic release of Daunorubicin from liposomal Daunorubicin hydrochloride in rabbits VX2 tumors, Int J Hyperthermia, 31:900-8.
6. Khatak S, Dureja H, 2017. Structural composition of solid lipid nanoparticles for invasive and non-invasive drug delivery, Curr. Nanomaterials, 2:129-53.
7. Shah M, Pathak K, 2010. Development and statistical optimization of solid lipid nanoparticles of simvastatin by using 23 full-factorial design, AAPS, Pharm. Sci. Tech, 11:489-96.
8. Gambhire S, Bhalekar R, Gambhire M, 2011. Statistical optimization of dithranol-loaded solid lipid nanoparticles using factorial design, Braz. J. Pharm. Sci, 47:503-11.
9. Yasir M, Sara S, 2014. Solid lipid nanoparticles for a nose to brain delivery of haloperidol, *in vitro* drug release and pharmacokinetics evaluation, Acta. Pharm. Sin. B, 4:454-63.
10. Bilati U, Allemann E, Doelker E, 2005. Development of a nanoprecipitation method intended for the entrapment of hydrophilic drugs into nanoparticles, Eur. J. Pharm. Sci, 25: Pp 67-75.
11. Dong Y, Ng W, Shen S, et al, 2012. Solid lipid nanoparticles: continuous and potential large-scale nanoprecipitation production in static mixers, Colloids Surf B, 94:68-72.
12. Costa P, Lobo S, 2001. Modeling and comparison of dissolution profiles, Eur. J. Pharm Sci, 13:123-33.
13. Gan L, Gao YP, Zhu CL, 2013. Novel pH-sensitive lipid-polymer composite microspheres of 10-hydroxycamptothecin exhibiting colon-specific biodistribution and reduced systemic absorption, J. Pharm. Sci, 102:1752-9.
14. Blasi P, Giovagnoli S, Schoubben A, 2011. Lipid nanoparticles for brain targeting formulation optimization, Int. J. Pharm, 419:287-95.
15. Bose S, Du Y, Takhistov P, et al, 2013. Formulation optimization and topical delivery of quercetin from solid lipid-based nano systems, Int. J. Pharm, 441:56-66.
16. Rajkumar M, Bhise B, 2010. Carbamazepine-loaded porous microspheres for short-term sustained drug delivery, J Young Pharm, 2:7-14.
17. Rahman Z, Zidan S, Khan A, 2010. Non-destructive methods of characterization of risperidone solid lipid nanoparticles, Eur. J. Pharm. Biopharm, 76:127-37.
18. Patel S, Chavhan S, 2011. Brain targeting of risperidone-loaded solid lipid nanoparticles by the intranasal route, J. Drug Target, 19:468-74.
19. Borgia L, Regehly M, Sivarama krishnan R, 2005. Lipid nanoparticles for skin penetration enhancement correlation to drug localization within the particle matrix as determined by fluorescence, J. Contr. Release, 110:151-63.
20. Cai S, Yang Q, Bagby R, et al, 2011. Lymphatic drug delivery using engineered liposomes and solid lipid nanoparticles, Adv Drug Delivery Rev, 10:901-8.

How to cite this article

N Dora Babu, 2022. Design and characterization of daunorubicin loaded solid lipid nanosuspension. J. Med. P'ceutical Allied Sci. V11 - I 1, Pages 4224 - 4432. doi: 10.55522/jmpas.V11I1.1389.